An empirical test of the role of small-scale transmission in large-scale disease dynamics

Joseph R. Mihaljevic[1,5*]

Carlos M. Polivka[2]

Constance J. Mehmel[3]

Chentong Li[1,6]

Vanja Dukic[4]

Greg Dwyer[1]

1. Department of Ecology and Evolution, University of Chicago, Chicago, IL 60637;

2. Pacific Northwest Research Station, USDA Forest Service, Wenatchee, WA 98801;

3. Okanogan-Wenatchee National Forest, USDA Forest Service, Wenatchee, WA 98801;

4. Department of Applied Mathematics, University of Colorado, Boulder, CO 80309;

5. School of Informatics, Computing, and Cyber Systems, Northern Arizona University, Flagstaff, AZ 86011;

6. School of Mathematics and Statistics, Xi'an Jiaotong University, Xi'an Shaanxi P.R.China 710049.

∗ Corresponding author; e-mail: joseph.mihaljevic@nau.edu.

Manuscript elements: Figure 1, figure 2, figure 3, figure 4, figure 5, table 1, table 2, table 3, online appendices A (including figure A1 through figure A9 and table A1 through table A4).

Keywords: Disease ecology, epidemiological modeling, Bayesian inference, microbial control.

Manuscript type: Article.

The authors wish to be identified to the reviewers.

Abstract

A key assumption of models of infectious disease is that population-scale spread is driven by transmission between host individuals at small scales. This assumption, however, is rarely tested, likely because observing disease transmission between host individuals is non-trivial in many infectious diseases. Quantifying the transmission of insect baculoviruses at a small scale is in contrast straightforward. We fit a disease model to data from baculovirus epizootics (= epidemics in animals) at the scale of whole forests, while using prior parameter distributions constructed from branch-scale experiments. Our experimentally-constrained model fits the large-scale data very well, supporting the role of small-scale transmission mechanisms in baculovirus epizootics. We further compared our experimentally-based model to an unconstrained model that ignores our experimental data, serving as a proxy for models that include large-scale mechanisms. This analysis supports our hypothesis that small-scale mechanisms are important, especially individual variability in host susceptibility to the virus. Comparison of transmission rates in the two models, however, suggests that large-scale mechanisms increase transmission compared to our experimental estimates. Our study shows that small-scale and large-scale mechanisms drive forest-wide epizootics of baculoviruses, and that synthesizing mathematical models with data collected across scales is key to understanding the spread of infectious disease.

Introduction

A fundamental assumption in much of theoretical ecology is that population rates of change are driven by interactions between individual organisms (Levin, 1992). This assumption is especially important in models of host-pathogen and host-parasite interactions, in which disease dynamics are assumed to be driven by transmission from infected to susceptible hosts (Keeling and Rohani, 2008). In these models, infection rates are quite sensitive to small changes in the pathogen or parasite's transmission rate. Tests of whether individual interactions drive disease dynamics in nature could therefore provide insight into fundamental issues in the ecology of disease.

A long-standing method of carrying out such tests is to estimate model parameters from observations of individual organisms at small spatial and temporal scales, and then to compare the resulting model predictions to data on population dynamics collected at large scales (Grimm et al., 2005; Kareiva and Odell, 1987). Agreement between model predictions and population-scale data is then taken as confirmation that individual interactions help explain disease dynamics, on the grounds that such agreement is unlikely to occur by chance.

For many host-pathogen and host-parasite systems, however, efforts to carry out this type of test face substantial logistic obstacles. Robust tests of the models require estimates of pathogen or parasite transmission rates at small scales, under natural conditions. In many host-pathogen and host-parasite systems, however, measuring transmission at small scales in nature is logistically impossible (McCallum et al., 2001).

Previous efforts have therefore instead typically estimated transmission rates either from large-scale data (Blackwood et al., 2013; George et al., 2011; Keeling et al., 2001; Murdoch et al., 2005), or from laboratory experiments (Buhnerkempe et al., 2011). In this previous work, most other parameters have been estimated from small-scale data, and the models have often succeeded at reproducing large-scale data, leading to significant insight into disease dynamics. It is nevertheless true that large-scale data do not necessarily reflect small-scale mechanisms, while laboratory experiments may not encompass the full range of mechanisms that affect pathogen or

parasite transmission in nature.

For insect baculoviruses, more complete tests may be possible, because measuring transmission at a small scale under natural conditions is straightforward (Elderd, 2013). In many insects, baculovirus transmission occurs when uninfected larvae, while feeding on host-plant foliage, inadvertently consume infectious occlusion bodies released from the cadavers of dead conspecifics (Cory and Hoover, 2006). Because larval insects are small and have limited mobility, it is possible to use field experiments to estimate baculovirus transmission rates at the scale of individual branches (Elderd, 2013). Compared to laboratory experiments, estimates of transmission rates from field experiments are more likely to reflect mechanisms that occur in nature (Cory and Hoover, 2006). Moreover, some baculoviruses attack insects that defoliate economically valuable tree species (Myers, 1988), and so pest managers often quantify epizootic severity (epizootic = epidemic in an animal) at the scale of entire forests (Moreau and Lucarotti, 2007). Large-scale data are thus also often available. It is therefore possible to estimate transmission parameters using data from experiments on branches, and to test the resulting model predictions using data from observations in entire forests.

As in disease ecology in general, the baculovirus literature regularly assumes that epizootics at the scale of forests can be explained by transmission at the scale of branches (Cory and Myers, 2003). There are nevertheless several larger-scale mechanisms that may modulate baculovirus dynamics. These mechanisms include differences in host density between branches or trees (Dwyer and Elkinton, 1993), variation in foliage quality across tree species, that can affect larval susceptibility (Elderd et al., 2008), and spatial variation in the frequency of pathogen strains (Fleming-Davies et al., 2015). Each of these mechanisms is manifest at larger spatial and temporal scales than the scale at which baculovirus transmission occurs between individual hosts.

To test the extent to which interactions between individuals can explain baculovirus epizootics, we used a branch-scale field experiment to estimate the transmission rate of a baculovirus of the Douglas-fir tussock moth, *Orgyia pseudotsugata*. We then generated model predictions by inserting our branch-level estimates of model parameters into mechanistic models of disease

spread, and we compared these predictions to epizootic data collected at the scale of entire forests. This approach has traditionally been implemented using only point estimates of model parameters (Buhnerkempe et al., 2011; George et al., 2011; Grimm et al., 2005; Keeling et al., 2001; Longini et al., 2005; Murdoch et al., 2005). Parameter uncertainty for disease models, however, is often substantial. This is important because the nonlinearities inherent in species interactions can cause small changes in estimates of model parameters to lead to substantial changes in model predictions, and thus in goodness of fit (Elderd et al., 2006). A lack of consideration of parameter uncertainty can therefore lead to inaccurate assessments of a model's goodness of fit.

To avoid this problem, we fit our models to both our small-scale experimental data and to large-scale epizootic data. We used a Bayesian statistical approach, so that it was at least possible that the epizootic data would dominate the fit of the model. In practice, however, the fit of the model was strongly constrained by the experimental data, so that our estimates of the model parameter values were fairly close to our estimates from the experimental data alone. Calculation of r^2 values then showed that the model that was fit to both types of data provides a good fit to the epizootic data, supporting the hypothesis that large-scale baculovirus epizootics are driven by interactions between individual hosts.

An absolute goodness of fit statistic like r^2, nevertheless, has limited usefulness, because small amounts of variation in the model parameters may have dramatic effects on the model's goodness of fit (Bolker, 2008). More broadly, the literature in this area has often emphasized model validation (George et al., 2011; Keeling et al., 2001). Although validation may be crucial for convincing environmental managers of a model's reliability, Box (1979)'s famous dictum is that "all models are wrong but some models are useful". Validation may therefore be of more limited usefulness in basic research than in applied research.

We therefore carried out a second test of the importance of individual interactions. In this second test, we compared the model that used parameters based on experimental data to a model in which all parameters were fit to the epizootic data alone (we follow Bayesian convention in referring to these cases as different models, even though the underlying differential equations

are identical). The model that was fit only to the epizootic data was thus unconstrained by the experimental data, allowing for the possibility that its parameter values would reflect the effects of large-scale phenomena. For example, if insects are clumped within trees, then the effective transmission rate might be higher than expected from a branch-scale measure of transmission. This higher level of transmission would then be reflected in a higher transmission parameter for the unconstrained model. Our unconstrained model thus serves as a proxy for more complex models. The unconstrained model is therefore of only moderate biological interest, but it provides a useful comparison to the models based on experimental data.

Because the unconstrained model was fit only to the epizootic data, it necessarily provides a better absolute fit to the data. The improvement in the fit was modest, however, providing additional support for the hypothesis that small-scale mechanisms drive epizootics. Some of the best-fit parameters for the two models were nevertheless quite different, and these differences suggest a more complex picture. Specifically, the estimate of the transmission rate from the unconstrained model is substantially higher than its experimental estimate, indicating that large-scale mechanisms affect transmission. In contrast, the estimate of variation in host infection risk from the unconstrained model is very similar to its experimental estimate, indicating that differences between individual hosts strongly affect epizootics. These comparisons are supported by model selection using the Watanabe-Akaike Information Criterion (WAIC, Gelman et al. (2014)). We therefore conclude that the transmission of the tussock moth baculovirus is driven by small-scale mechanisms, but that large-scale mechanisms likely also play a meaningful role. As we discuss, this result has broad implications for our understanding of host-pathogen interactions.

Methods

Baculovirus Natural History

The models that we use were first developed for human pathogens (Anderson and May, 1992), but are general enough that they can be used to describe baculovirus epizootics. To explain why,

we first describe baculovirus natural history, and then we show how simple SEIR models can encompass this natural history.

Baculovirus epizootics play a key role in terminating tussock moth outbreaks, which occur at roughly 10-year intervals (Mason, 1996). During outbreaks, tussock moth densities increase from levels at which larvae are undetectable, to levels at which defoliation may be widespread and severe (Shepherd et al., 1988). Outbreaking populations are reliably terminated by baculovirus epizootics, in which cumulative mortality can exceed 90% (Mason, 1996). So far as can be known, the Douglas-fir tussock moth is the only organism in its range that is susceptible to the baculovirus, although *Orgyia* species from other parts of North America have been successfully infected with the Douglas-fir tussock moth baculovirus in the lab (Rohrmann, 2014).

As we mentioned, transmission occurs when larvae incidentally consume infectious virus particles known as "occlusion bodies" while feeding on foliage (Cory and Myers, 2003). Larvae that consume a large enough dose die in about two weeks. Shortly after death, viral enzymes dissolve the insect's integument, releasing occlusion bodies onto the foliage, where they are available to be consumed by additional larvae (Miller, 1997). Epizootics are terminated when larvae pupate, or when epizootics are so severe that most hosts die before pupating (Fuller et al., 2012).

The virus overwinters largely through external contamination of egg masses (Thompson and Scott, 1979). The rate of egg-mass contamination therefore determines infection rates at the beginning of the larval period, which are often low (Otvos et al., 1987). High infection rates then apparently result from multiple rounds of transmission during the larval period (Otvos et al., 1987; Shepherd et al., 1984). In our study areas in Washington, Idaho, and Colorado, USA, and British Columbia, Canada, the larval period is currently early June to mid-August.

A Random SEIR Model

Because pathogen transmission and host reproduction occur at different times of the year, we described baculovirus epizootics using a model that does not include host reproduction. We

began with a standard Susceptible-Exposed-Infectious-Recovered or "SEIR" model from human epidemiology (Keeling and Rohani, 2008), and we modified the model to allow for heterogeneity in host infection risk. In our model, heterogeneity in infection risk includes a stochastic component that reflects the effects of weather, and a deterministic component that reflects inherent differences between hosts. The model is:

$$\frac{dS}{dt} = -\bar{\nu}e^{\epsilon_\tau} SP \left[\frac{S(t)}{S(0)}\right]^{C^2}, \tag{1a}$$

$$\frac{dE_1}{dt} = \bar{\nu}e^{\epsilon_\tau} SP \left[\frac{S(t)}{S(0)}\right]^{C^2} - m\delta E_1, \tag{1b}$$

$$\frac{dE_i}{dt} = m\delta E_{i-1} - m\delta E_i \quad (i = 2, \ldots, m), \tag{1c}$$

$$\frac{dP}{dt} = m\delta E_m - \mu P. \tag{1d}$$

As in standard SEIR models, transmission occurs through a mass action term. In models of human diseases, this term is often written as βSI, where S is the density of uninfected or "susceptible" hosts, I is the density of infected hosts, and β is the transmission parameter. Here transmission instead occurs through contact between susceptible hosts and infectious cadavers P, with transmission parameter $\bar{\nu}$.

We further modify the transmission term to allow for inherent variation among hosts in their susceptibility to the pathogen, according to $\left[\frac{S(t)}{S(0)}\right]^{C^2}$. This term comes from models originally developed for the gypsy moth baculovirus (Dwyer et al., 1997), which were in turn derived from models of sexually transmitted infections in humans (Anderson and May, 1992). The approach is to assume that there is a distribution of infection risk in the host, with mean $\bar{\nu}$ and coefficient of variation C, where individual infection risk is represented by the transmission rate ν (Dwyer et al., 2000). The resulting model is an approximation to a more computationally intensive partial-differential equation model. The approximation is highly accurate if transmission rates follow a gamma distribution, but it is also reasonably accurate if transmission rates instead follow a log-normal distribution, which has a fatter tail than a gamma distribution (G. Dwyer, unpublished). In general, we assume that transmission occurs among larvae in the fourth instar (= larval

stage), the instar that has the biggest impact on cumulative infection rates (Dwyer, 1991; Otvos et al., 1987). To allow for the smaller size of hatchlings, we multiply the initial virus density by the parameter, ρ, which is the ratio of the number of virus particles produced by a first-instar cadaver to the number produced by a fourth-instar cadaver.

In referring to "inherent variation", we are making a distinction from daily variation in insect feeding behavior (Lance et al., 1986), which can respond in complex ways to variation in weather (Eakin et al., 2015). To represent daily variation, we include a random variate ϵ_τ, which modifies the transmission rate each day τ, where τ is an integer that indicates the day during the epizootic. The value of ϵ_τ for each day τ is drawn from a normal distribution with mean 0 and standard deviation σ. By exponentiating ϵ_τ, we eliminate the possibility of negative transmission, which would be biologically meaningless.

Including ϵ_τ is important because stochasticity may interact in complex ways with disease dynamics, so that the variability in the model predictions changes as the epizootic proceeds, or as initial host and pathogen densities vary between epizootics. By including stochasticity, we allow for this type of variation, ensuring that our estimation procedures are statistically robust. Because weather conditions likely varied between populations, we estimated a value of the standard deviation σ for each epizootic.

As in standard SEIR models, susceptible hosts S that become infected proceed through m exposed classes, E_i. Exposed hosts eventually die of the infection, joining the infectious-cadaver class P (the R class of SEIR models corresponds to cadavers that are no longer infectious, and so we do not include it here). Cadaver infectiousness decays at rate μ, due mostly to UV radiation (Thompson and Scott, 1979). Hosts move between exposed classes at rate $m\delta$, so that the time spent in a single exposed class follows an exponential distribution with mean time $1/(m\delta)$. The total time in the m exposed classes is the sum of m such distributions, and a well-known theorem has shown that this sum follows a gamma distribution with mean, $1/\delta$, and variance, $1/(m\delta^2)$ (Keeling and Rohani, 2008).

A well known approach to allowing for stochasticity in ordinary differential equations (ODEs)

assumes that stochastic perturbations occur over infinitesimal time scales, leading to "stochastic ODEs" (Øksendal, 2003). Because we instead assume that stochastic perturbations occur over a finite (daily) time scale, our model equations are instead known as "random ODEs" (Han and Kloeden, 2017). The distinction is important because, as we explain in the Online Appendix, numerical integration of random ODEs can rely on methods from deterministic calculus (Han and Kloeden, 2017). Numerical integration of stochastic ODEs in contrast requires more sophisticated methods (Øksendal, 2003).

Field transmission experiments

In equations (1a)-(1d), the average transmission rate, $\bar{v}$, represents the overall infection risk per unit time. It therefore encompasses both the probability of exposure and the probability of infection given exposure, allowing for the effects of both host behavior and host-tree foliage quality. Accordingly, $\bar{v}$ is best measured using field experiments, in which larvae feed freely on virus-contaminated foliage (Elderd, 2013).

Previous work with the gypsy moth, *Lymantria dispar*, produced a protocol for baculovirus field-transmission experiments that gives repeatable results (Dwyer, 1991; Dwyer et al., 1997; Fleming-Davies et al., 2015). Following this protocol, we first reared uninfected tussock moth larvae in the laboratory from field-collected egg masses. The egg masses had been collected from an early-stage outbreak in Cheyenne Mountain State Park in Colorado, USA, in 2014. To deactivate any virus particles on the surface of the eggs, we submerged the egg masses in 5% formalin for 90 minutes prior to incubation (Dwyer and Elkinton, 1995). We used hatchling larvae as infected hosts in our experiments because the most important round of transmission occurs when third and fourth instar larvae are infected by first instar cadavers (Otvos et al., 1987; Shepherd et al., 1984).

To infect the hatchlings, we placed them on artificial diet contaminated with the virus. A pilot study allowed us to determine the viral dose that results in $\sim$95% of larvae becoming infected. We therefore used a solution of 10^4 occlusion bodies/μl, and we used a Pasteur pipette to place

5 drops of this solution onto artificial diet in a 6 oz (177 ml) plastic rearing cup. After feeding for 24h, larvae were moved to additional rearing cups.

To ensure that the infected larvae were indeed infected, we reared them at 26 °C in the laboratory for five days. Five days was long enough to ensure that any uninfected larvae would molt to the second instar, whereas the virus prevented infected larvae from molting (Burand and Park, 1992) . This made it easy to identify and remove uninfected larvae (Fuller et al., 2012). The infected larvae were then placed on Douglas-fir branches in the field at two densities, 10 and 40 larvae per branch. The trees that we used were encompassed within an area of roughly 2 hectares in the Okanogan-Wenatchee National Forest, near Entiat, Washington, USA.

The branches were enclosed in mesh bags, which prevent the emigration of larvae and the breakdown of the virus (Fuller et al., 2012). We then allowed the infected larvae to disperse on the foliage and die, which takes roughly 5 days. On the fifth day, we added 20 uninfected larvae, which we had reared in the lab to the fourth instar (Dwyer et al., 1997). Controls consisted of branches containing only uninfected larvae.

An insect larva's susceptibility to baculovirus infection can vary in a complex way within an instar (Grove and Hoover, 2007). We therefore developmentally synchronized the uninfected fourth instars. Shortly before molting, a larva's head capsule slips forward, making it possible to see that the larva is close to the end of its instar. To synchronize fourth instars, we collected third instars with slipped head capsules, and we held them at 4°C, halting development, until we had enough larvae to begin the experiment. We then reared the larvae at 26°C until they had molted to the fourth instar, which occurred within 48 hours. This protocol produced larvae that had reached the fourth instar within a relatively short period. In previous experimental data generated by using this protocol, the variance in the infection rate has been indistinguishable from the variance of the corresponding binomial distribution (Elderd et al., 2008). Synchronization therefore appears to eliminate most sources of extraneous variability, leaving only the binomial variation that is expected in an infection experiment.

Our experimental treatments consisted of the 2 viral densities (10, 40), crossed with 3 viral

isolates, for a total of 6 treatments, each replicated 14 times. We also established 7 control bags, in which there were no infectious cadavers. The WA isolate was collected from Washington State in 2010, while the NM isolate was collected in New Mexico in 2014. The final isolate was TMB-1 ("Tussock Moth Bio-control 1"). This isolate makes up the insecticidal spray formulations produced by the USDA Forest Service (Martignoni, 1999), which is often used to control outbreaking tussock moth populations. Transmission electron microscopy showed that all three isolates were the multicapsid form of the virus, known as "*Op*MNPV". In multi-capsid strains, the virions are found in clumps within the occlusion bodies, as opposed to single-capsid (*Op*SNPV) strains, in which the virions occur singly within the occlusion bodies (Hughes and Addison, 1970).

The experiment included 91 branches with 20 uninfected larvae each, for a total of 1,820 uninfected larvae. We allowed the initially uninfected larvae to feed on foliage for 7 days, and then we removed the branches from the trees and brought them into the laboratory. Next, larvae from the branches were reared individually for three weeks in 2 ounce (59 ml) cups partially filled with artificial tussock moth diet, at 26 °C in the laboratory. To determine if larvae had died of the virus, we examined smears from dead larvae under a light microscope at 400× for the presence of occlusion bodies, which are easily visible at that magnification (Fleming-Davies et al., 2015).

After the 7 day experimental period, we photographed each branch, and we used ImageJ (Schindelin et al., 2015) to estimate the area of foliage on each branch. We then calculated the density of infectious cadavers and the density of uninfected hosts by dividing the number of cadavers or hosts by the foliage area. This allowed us to measure densities on single branches using the same units as in the epizootic data, with the proviso that the epizootic data were collected at a scale of 1-10 hectares.

As part of this experiment, we attempted to measure the decay rate μ of infectious cadavers on foliage, by allowing some cadavers to be exposed to sunlight outside of the mesh bags for 3 days. 3 days, however, proved to be too short a period for us to detect meaningful decay of the virus, and we therefore do not report those results. Previous work was similarly unsuccessful at

estimating the decay rate of the tussock moth baculovirus when using exposure periods of 1, 4, 13, and 32 days (Dwyer, 1992). It may therefore be that the decay rate of the virus is very low. As we will show, this result is consistent with some of the estimates of the decay rate μ that result from fitting our models to the epizootic data.

Estimating Transmission Parameters From the Experimental Data

The mesh bags that enclosed the experimental branches prevented the emigration of larvae and the breakdown of the virus, and the experiment was short enough that no larvae became infected and then died during the experiment. The density of infectious cadavers on the experimental branches was therefore constant after the experiment began. Also, given the short duration and small spatial scale of our experiment, it is reasonable to assume that transmission stochasticity is negligible. We can then set the infectious cadaver density $dP/dt \equiv 0$ in equation (1d), which in turn makes it possible to solve the host equation (1a) for the density of hosts S that remain uninfected at the end of the experiment, as a function of the virus density P_0 (Dwyer et al., 1997). For purposes of comparison to data, it is useful to write this expression in terms of the log of the fraction uninfected $(1-i)$:

$$-\log(1-i) = \frac{1}{C^2}\log\left(1 + C^2\bar{\nu}P_0\hat{t}\rho\right) \tag{2}$$

Here, $\hat{t}$ is the time larvae were exposed to virus on foliage, which was 7 days. The ratio parameter, ρ, is included because an implicit assumption of the SEIR model is that all larvae are in the fourth instar, but the infectious cadavers in our experiment were in the first instar. The parameter ρ therefore scales the transmission rate so that it is expressed in terms of fourth-instar cadavers. We also allowed for the possibility that host heterogeneity C was negligible, which instead gives the model:

$$-\log(1-i) = \nu P_0\hat{t}\rho. \tag{3}$$

To estimate values of transmission $\bar{\nu}$ and heterogeneity C, we used the Bayesian inference software, *JAGS* (http://mcmc-jags.sourceforge.net/) via the *rjags* package in `R`. We assumed vague

priors for $\bar{v}$ and C, and an experimentally-derived prior for the ratio parameter ρ, as we will describe. To avoid biases in the parameter estimates, we explicitly allowed for error in the cadaver densities P_0 in the statistical model. We then compared the full and nested models using WAIC (see Online Appendix for the definition of WAIC). Example code for the fitting routine for this model is provided in the Online Appendices.

Seven of our 91 experimental branches had 100% mortality due to desiccation. Desiccation is a common source of natural mortality in Douglas-fir tussock moth populations (Mason and Torgersen, 1983), but it may have been slightly worse in our case because the mesh bags can elevate temperatures (Páez et al., 2017). We therefore excluded these seven branches from our analyses. We also excluded desiccated larvae from the other branches, partly because desiccated larvae were too dry to be autopsied, but more importantly because desiccated larvae were unlikely to have been infected. The estimated 2-dimensional area of foliage per replicate branch ranged from 0.09 to 0.28 m^2 (mean = 0.15). After correcting for this variability, the cadaver density for the low density treatment (10 cadavers per branch) ranged from 38.49 to 112.58 cadavers per m^2 of foliage (mean = 70.58), and the high density treatment (40 cadavers per branch) ranged from 142.38 to 426.98 cadavers per m^2 of foliage (mean = 254.41).

Other Types of Experimental Data

We also used an experiment to estimate the average speed of kill, which in the model is equivalent to $1/\delta$, the inverse of the death rate. In this experiment, we infected larvae by allowing them to feed on Douglas-fir foliage that was contaminated with a sprayed virus solution (Online Appendices). For logistical convenience, this experiment was carried out in the laboratory. Because speed of kill is affected by temperature, we were careful to hold the larvae at temperatures typical of field conditions (Polivka et al., 2017).

To estimate the ratio parameter, ρ, we again infected larvae in the laboratory, but in this case we infected both hatchlings and fourth instars (Online Appendices). We held these larvae in the laboratory until death or pupation, and we counted the number of occlusion bodies per dead

larva for each instar, using a hemocytometer under a light microscope.

The Epizootic Data

Because the tussock moth baculovirus is effectively species specific, it has often been used as an environmentally benign insecticide, to reduce defoliation damage imposed by outbreaking tussock moth populations (Otvos et al., 1987). Our epizootic data therefore came from 7 unsprayed control plots and 5 sprayed treatment plots, and included both published data, and data that we present here for the first time. Although the TMB-1 isolate used in the spray formulation may be phenotypically different than wild-type virus, fitting models with different transmission rates for spray and control plots showed that the transmission rates of TMB-1 and wild-type virus are effectively indistinguishable (Mihaljevic et al., 2019).

In spray programs, managers typically establish control plots in the same general area as spray plots, but far enough away to prevent sprayed virus from drifting into control plots. The data from Washington State were thus from a spray program in 2010, in which all plots were at least 10 kilometers apart. This distance is far enough that drift of the virus spray was vanishingly unlikely. The data from British Columbia were similarly from a spray program in 1982 (Otvos et al., 1987), but some plots were only a few hundred meters apart. In the control plots, however, the epizootics started 3-4 weeks later than in the treatment plots. Given that sprayed virus typically decays within a few days (Polivka et al., 2017), this time lag suggests that drift of the spray was again minimal.

At the beginning of the larval period at each site, initial host and pathogen population densities were estimated using standard methods, which provided initial conditions for our models (Online Appendices). Because initial virus densities in sprayed treatment plots were much higher than in unsprayed control plots, the two types of epizootic data together encompass a broader range of initial pathogen densities than either type of epizootic data alone. This is important because a broad range of densities often increases statistical power when ecological models are fit to data (Pascual and Kareiva, 1996).

The data consist of approximately weekly observations of the fraction of larvae infected with the virus, for up to 50 days, or approximately mid-June to mid-August. In the sprayed plots, insects were collected within 7 days after application of the virus, while in the control plots, the start of collections was more variable, particularly at sites where there was no concurrent spray project. Collected insects were reared and diagnosed as they were in the field transmission experiment.

Model fitting and model selection

To fit models to the epizootic data, we compared the fraction infected in the data to the fraction infected in the model. In the model, infected (but not yet dead) larvae are represented by the exposed classes E_m. The fraction infected is then $\frac{\sum E_m}{\sum E_m + S}$.

For the transmission data, we used a binomial likelihood function, but for the epizootic data, a binomial likelihood function was unlikely to be sufficient. Use of a binomial distribution rests on the assumption that individual hosts are independent (McCullagh and Nelder, 1989). It seems likely that, in epizootics, this assumption might not be correct, because it is not unlikely that hosts with higher-than-average infection risk, or lower-than-average infection risk, are clustered within the forest. Such clustering could cause the variance in the infection risk to be substantially higher than the variance of the corresponding binomial, a phenomenon known as over-dispersion.

In the absence of direct information on the level of over-dispersion, a useful approach is to use a beta-binomial distribution (Cox and Snell, 1989). In a beta-binomial distribution, the binomial probability of an infection p follows a beta distribution, which describes quantities that vary between 0 and 1. The resulting beta-binomial has two parameters, as opposed to the single parameter of the binomial. Using a beta-binomial allowed us to increase the variance as needed to explain the lack of fit of the model to the data (because our model is stochastic, we also allowed for the possibility that the lack of fit was due to stochasticity in transmission). As parameters of the beta-binomial, we used $a = pe^{\gamma}$ and $b = (1-p)e^{\gamma}$, where p is the model prediction of the fraction infected and γ is an inverse measure of the over-dispersion. As we will show,

over-dispersion levels were moderate but not excessive.

Because our epizootic models allow for stochastic fluctuations in transmission, we integrated likelihood values over many realizations of the models. This approach is equivalent to integrating out the values of the stochasticity ϵ_τ, leading to an average value of the likelihood:

$$\bar{L} = \int L\left(\epsilon_1, \epsilon_2, \ldots, \epsilon_D\right) f\left(\epsilon_1, \epsilon_2, \ldots, \epsilon_D\right) d\epsilon_1 d\epsilon_2 \ldots d\epsilon_D \tag{4}$$

Here, $\bar{L}$ is the average likelihood, and D is the number of days in an epizootic, and thus the number of days for which we drew ϵ_τ values. The function $f\left(\epsilon_1, \epsilon_2, \ldots, \epsilon_D\right)$ is the probability density of the ϵ_τ's, where each integer, $1, 2, \ldots, D$, indicates a different day.

Numerical integration of the model is computationally expensive, and so using numerical quadrature to calculate the integral in equation (4) is impractical. We therefore instead used Monte Carlo integration (Ross, 2002). This meant drawing values of the ϵ_τ's, and then calculating the average likelihood;

$$\hat{\bar{L}} \quad = \quad \frac{1}{R} \sum_{j=1}^{R} L(\epsilon_1^j, \epsilon_2^j \ldots \epsilon_D^j). \tag{5}$$

Here R is the number of realizations, and ϵ_1^j is the value of ϵ_1, meaning the stochastic term on day 1, in the jth realization. According to the weak law of large numbers, as $R \to \infty$, $\hat{\bar{L}} \to \bar{L}$ (Ross, 2002).

To reduce computing time, it was important to ensure that $\hat{\bar{L}}$ approached $\bar{L}$ for a reasonably small number of realizations. For this purpose we used the MISER Monte-Carlo integration algorithm. This algorithm uses recursive, stratified sampling to estimate the average likelihood, while minimizing the number of realizations. Briefly, the algorithm works as follows (the code that we use is from the Gnu Scientific Library, but for a more complete explanation, see Press et al. (1992)). As equation (5) shows, in calculating an estimate of the average likelihood $\hat{\bar{L}}$, we are sampling over a D-dimensional space of stochasticity parameters ϵ_τ. Within this parameter space, it is likely that there are sub-spaces within which the variance in $\hat{\bar{L}}$ is higher than in other sub-spaces. In estimating $\hat{\bar{L}}$ across the entire space, it turns out to be more efficient to sample

more frequently in sub-spaces within which the variance is higher. This proposition, which can be demonstrated formally, forms the basis of the MISER algorithm.

The algorithm is given a quota of R realizations. Some fraction of these realizations, in our case 0.1, is devoted to sampling uniformly across the entire space. Based on this initial sample, the algorithm recursively divides the overall space into sub-spaces of high and low variance. In using the remaining realizations, the algorithm then samples more intensively in sub-spaces of high variance. The end result is an estimate of $\hat{\bar{L}}$ that minimizes the variance. Initial trials with this algorithm showed that 150 realizations was generally sufficient to produce reliable estimates of $\hat{\bar{L}}$, in the sense that a larger number of realizations only reduced the variance in $\hat{\bar{L}}$ by a small amount.

We then used our likelihood in Bayes' theorem:

$$P(\theta|D) \quad \propto \quad \pi(\theta)\mathcal{L}(\theta|D). \tag{6}$$

Here $P(\theta|D)$ is the posterior probability of the parameters θ of a model that we are fitting to data D. The symbol $\pi(\theta)$ is the prior probability of the parameters, and $\mathcal{L}(\theta|D)$ is the likelihood of the parameters. Because in general posterior probabilities are only used for comparison purposes, we only need to calculate the posterior probability up to a constant of proportionality, hence our use of the proportion symbol $\propto$.

To create priors from our experimental data, we constructed log-normal prior probability distributions for transmission $\bar{v}$, heterogeneity C, and ratio ρ, from the marginal posterior samples generated from our analyses of the transmission data. On a log scale, the marginal posterior samples were well described by normal distributions, and so we constructed priors by calculating sample means and standard deviations from the posterior marginals. We expressed transmission heterogeneity C in terms of the parameter $k = 1/C^2$, because, on a log scale, k has a distribution that is more nearly normal than C. We similarly used our experimental data to construct a log-normal prior on the death-rate parameter δ.

Experimental data on speeds of kill typically show extremely low variance (Dwyer, 1991),

while using the epizootic data to estimate the number of exposed classes m, which determines the variance in the speed of kill, proved to be almost impossible. We therefore set $m = 200$ to ensure that the variance in the speed of kill was realistically low. The remaining model parameters are the decay rate μ, the stochasticity parameter σ, and the over-dispersion parameter γ. For these latter parameters, we used uniform probability distributions as "vague" priors, in which effectively all possible parameter values were equally likely, up to some large upper limit. Given that the "nuisance" parameters σ and γ determine the process error and the observation error respectively (Bolker, 2008), the only biologically interesting parameter that we estimated from the epizootic data alone was the cadaver decay rate μ.

Because our experimental and observational data sets are independent, we could have fit models to the data by adding the log likelihoods of the two data sets. Such an approach would be equivalent to carrying out maximum-likelihood estimation (Bolker, 2008). By instead using Bayes's theorem, we allowed for the possibility that the likelihood would dominate the experiment-based priors. It was therefore at least possible that our fitting routine would produce posterior parameter estimates that were far from the values calculated from our experiments.

For the model with experiment-based priors, however, the posterior median values of the parameters were reasonably close to the medians calculated from our experiments. This could have happened because the experiment-based priors provide an excellent fit to the epizootic data, but it could instead have happened because the epizootic data do not provide much information about the model and its parameters. In practice, both phenomena were operating, in the sense that the experiment-based priors provide a reasonable fit, and that, relative to the experimental data, the epizootic data provided only a moderate amount of information about the model parameters. To show this, we also fit a model for which all parameters had vague priors. In this model, the posterior medians of the heterogeneity parameter C, the ratio parameter ρ, and the death-rate parameter δ were again close to our experimental medians, but the posterior median of the transmission rate $\bar{v}$ was meaningfully different from its experimental median. This is important partly because $\bar{v}$ is in units of per cadaver$/m^2$, per day, and therefore reflects the scale at

which interactions occur.

In comparing posterior parameter distributions for the two models, we therefore also compared the two models more quantitatively, in two different ways. First, we calculated the coefficient of determination r^2 for each model. To define r^2, we first define $\mathrm{SS_{tot}}$ to be the total sum of squared errors across all observations in our data set:

$$\mathrm{SS_{tot}} = \sum_{i=1}^{n} (D_i - \bar{D})^2. \tag{7}$$

Here n is the total number of observations of the fraction infected in our data set, D_i is data point (fraction infected) i, and $\bar{D}$ is the average fraction infected across all epizootics. $\mathrm{SS_{tot}}$ is thus the total variation in the data set. $\mathrm{SS_{res}}$ is the residual sum of squares, defined as:

$$\mathrm{SS_{res}} = \sum_{i=1}^{n} \frac{1}{R} \sum_{j=1}^{R} (D_i - M_{i,j})^2 \tag{8}$$

Here we are averaging across $R = 500$ model realizations. $\mathrm{SS_{res}}$ then measures the error between the model and the data, and thus the extent to which the model reproduces the data. We then define r^2 according to,

$$r^2 = 1 - \frac{\mathrm{SS_{res}}}{\mathrm{SS_{tot}}}. \tag{9}$$

We thus use r^2 to calculate the fraction of the variance in the data that is explained by the model, or equivalently, the extent to which the model produces better predictions of the epizootic data than a prediction that is equivalent to the average fraction infected.

Because the model with vague priors was fit only to the epizootic data, its r^2 value will necessarily be as good or better than the r^2 values for models with experiment-based priors. As we mentioned, however, the improvement in the r^2 value was modest. An additional important question is therefore, does the model with vague priors provide a meaningfully better explanation for the epizootic data than the model with experiment-based priors? This is an important question to ask, because by fitting the unconstrained model to the epizootic data alone, we ran a serious risk of over-fitting the data.

A standard method of accounting for over-fitting is to use model selection. As a model selection criterion, we again used WAIC, because, in contrast to most model-selection criteria, WAIC is fully Bayesian (Gelman et al., 2014), and so it incorporates variability in both the model's prior and its posterior. WAIC therefore allowed us to quantify the effects of our experimental-based priors on the model's predictive ability (see the Online Appendix for a longer explanation of WAIC).

In most applications of model selection, the models being compared differ in structure. In our case in contrast, the model structure, as defined by the random ODEs in equations (1a)-(1d), is the same for all models. Our models therefore differ only in their prior probability distributions. We are thus using WAIC in an unconventional way, but to our knowledge there is no established method of choosing between models with different priors. This is true even though, as we described, estimating model parameters at a smaller scale than the test data is a common procedure in disease ecology, and using small-scale data to construct priors is one way to carry out this procedure in a way that allows for parameter uncertainty. We therefore argue that WAIC is useful in this context.

Moreover, as we will show, the results of our WAIC analysis confirm the results of our comparisons of posterior parameter estimates. That is, models with experiment-based priors on the transmission parameter fit the epizootic data substantially worse than models with vague priors on the transmission parameter. We therefore conclude that large-scale processes have at least some effect on the dynamics of this pathogen.

Results

Experiments

For two of the three strains that we tested, the best-fit model has a strongly nonlinear shape (fig. 1). The model with the best (lowest) overall WAIC score therefore includes host heterogeneity in infection risk (Table 2). Fig. 1 also shows that the three isolates differed strongly, such that

the NM isolate had much higher heterogeneity in transmission, while the WA isolate had much lower heterogeneity in transmission. These effects are reflected in the median posterior estimates of the values of heterogeneity C for the three isolates (Table 1).

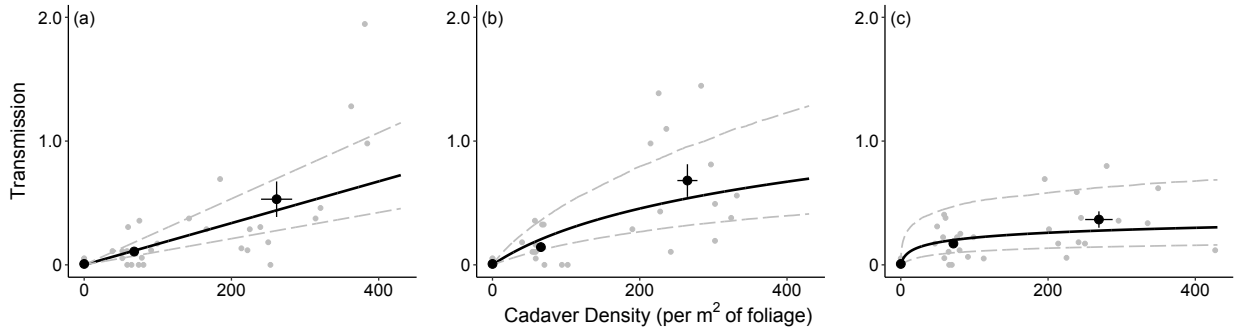

Figure 1: Results of the field transmission experiment, with (a) the WA isolate, (b) TMB-1, and (c) the NM isolate. In the figure, the solid lines represent the median model predictions, while the gray dashed lines represent boot-strapped 95% credible intervals. The large black points with error bars represent the mean and the standard error of the infection-rate and density data for the low cadaver density treatment, and the high cadaver density treatment, respectively. The small gray points represent the observed values on each branch.

Table 1 suggests that higher average transmission rates $\bar{v}$ were associated with higher variation in transmission C. With only 3 isolates, we cannot reach general conclusions, but in the gypsy moth baculovirus, more extensive data revealed a negative correlation between the average and the CV of transmission, consistent with this pattern (Fleming-Davies et al., 2015). A similar correlation may therefore occur in the tussock moth baculovirus. More immediately, the variation across isolates is important when we use our experimental data to explain the epizootic data, because in the epizootic data, we have no information about the isolates that were present. In constructing informative priors from our experimental data, we therefore allowed for uncertainty due to isolate variation by pooling the marginal posterior distributions for the three isolates, and inflating the pooled variance slightly (Online Appendices).

Isolate	Average transmission, $\bar{v}$	Host heterogeneity, C
WA	0.006 (0.003, 0.010)	0.60 (0.05, 1.52)
TMB-1	0.012 (0.004, 0.030)	1.52 (0.25, 2.51)
NM	0.076 (0.005, 3.104)	4.11 (2.15, 6.45)

Table 1: Best-fit transmission parameters (average transmission, $\bar{v}$, and heterogeneity, C) for three viral isolates. Values are posterior medians with 95% credible intervals. Units on $\bar{v}$ are per infected cadaver/m^2, per day. Heterogeneity is the squared C.V. of the distribution of infection risk, and its units are therefore meaningless.

Model Type	WA Isolate	NM Isolate	TMB-1	Overall
$\boldsymbol{C > 0}$	175.53	**179.48**	**165.06**	**520.07**
$C = 0$,	174.28	199.11	168.45	541.84

Table 2: Model selection for the transmission experiment. The bold-faced WAIC scores highlight the best model, based on ΔWAIC > 3.

Comparing Models to the Epizootic Data

In the epizootic data, initial infection rates in controls were low, but increased slowly over the larval period (fig. 2). In populations with low initial host densities, it took weeks for the infection rate to reach high levels. Sprayed sites in contrast received an initial inundation of the pathogen, and so infection rates in those sites increased within a week or two after the spray application. Host population collapse was therefore rapid in the sprayed sites, leading to weaker effects of initial host density.

The model with experiment-based priors generally does an excellent job of reproducing the epizootic data (fig. 2), with $r^2 = 0.68$. This model thus uses our experimental data, collected at a the spatial scale of a roughly 0.1 m^2 of foliage over a temporal scale of 7 days, to predict epizootic data, collected at a scale of 1-10 hectares over as many as 50 days. The model is therefore extrapolating over 5-6 orders of magnitude in spatial scale and a factor of 3-7 in temporal scale,

with some success. Meanwhile, the model with vague priors does only a slightly better job of reproducing the epizootic data (fig. 3), with $r^2 = 0.75$. Notably, levels of over-dispersion were non-zero but moderate for both models (Online Appendices). The performance of the model with experiment-based priors therefore suggests that transmission at a small-scale is an important driver of epizootics at a large scale.

This positive picture is altered when we consider the posterior estimates of the model parameters. For both the model with experiment-based priors and the model with vague priors, the posterior distributions of the heterogeneity parameter C, the ratio parameter ρ, and the speed of kill parameter δ strongly overlap with the corresponding posteriors from the experimental data (fig. 4). For the model with vague priors, the posterior median of ρ is moderately lower than the experimental median for the model with experiment-based priors. For models with intermediate numbers of experiment-based priors, the posterior distributions of these three parameters also strongly overlap with the experimental posteriors (Online Appendix) These results suggest that our experimental estimates of heterogeneity C, the ratio parameter ρ, and the death rate parameter δ are all reasonably accurate, compared to estimates that take into account epizootic data.

For the transmission rate $\bar{v}$, however, the median posterior for the model with experiment-based priors is roughly an order of magnitude higher than the experimental median. For the model with vague priors, the posterior median of $\bar{v}$ is almost two orders of magnitude higher than the experimental median, and there is no overlap in the 95% credible intervals of the two distributions (fig. 4). For models with experiment-based priors on parameters other than $\bar{v}$, the posterior medians of $\bar{v}$ are also substantially higher than the experimental estimate (fig. 5).

Our WAIC analyses are consistent with these results. As Table 3 shows, the model with vague priors provides the best explanation for the epizootic data. For three models with experiment-based priors on parameters other than transmission $\bar{v}$, ΔWAIC scores are less than 3, and thus the fit of these models is effectively indistinguishable from the fit of the best model. In the Online Appendices, we show that the visual fit of these models to the data is very similar to the

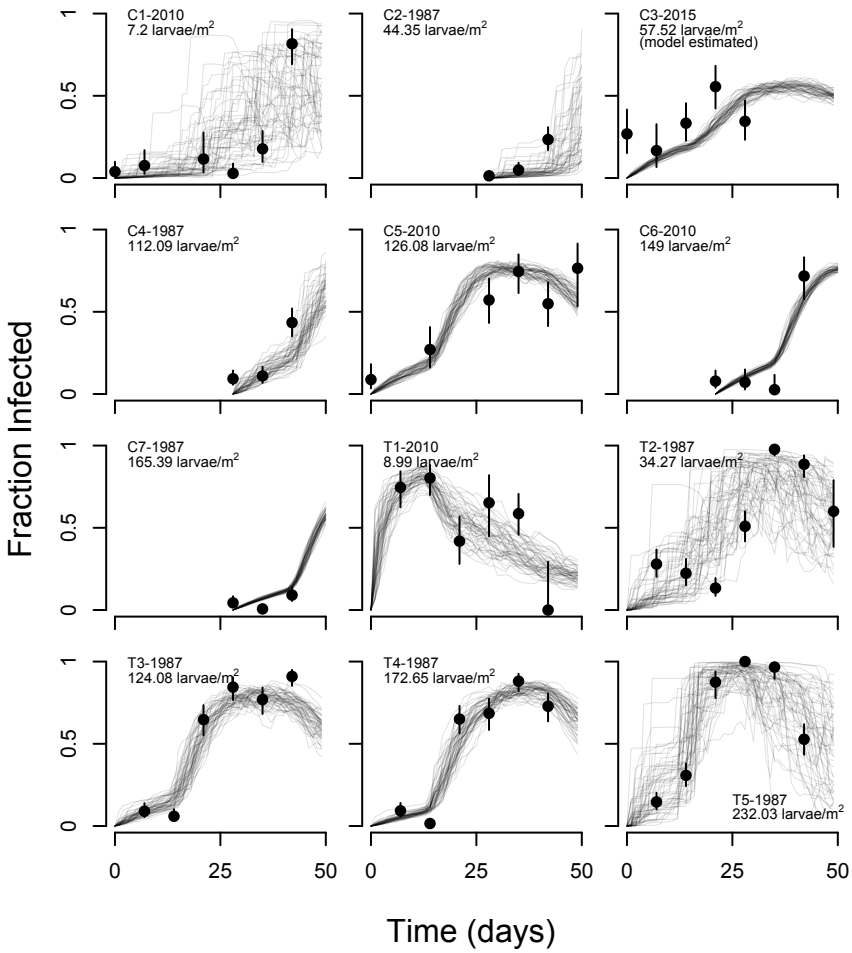

Figure 2: Stochastic realizations of the model with informative priors on $\bar{v}$, C, ρ, and δ, versus the data (black points with 95% binomial confidence intervals as error bars). The labels C and T stand for Control and Treatment (meaning treated with virus spray), respectively, and are followed by the year of observation. The initial larval host density is also shown. Note that for the Colorado site (C3-2015), the initial larval host density was estimated from the data. Here and in subsequent figures, for two of the populations (C3-2015, C4-1987), we show the model's predictions after the last data point was collected, to illustrate the overall dynamics of the pathogen.

visual fit of the best model with all vague priors. For models with experiment-based priors on transmission $\bar{v}$, however, WAIC scores are meaningfully worse than for the model with vague priors, with ΔWAIC > 5.

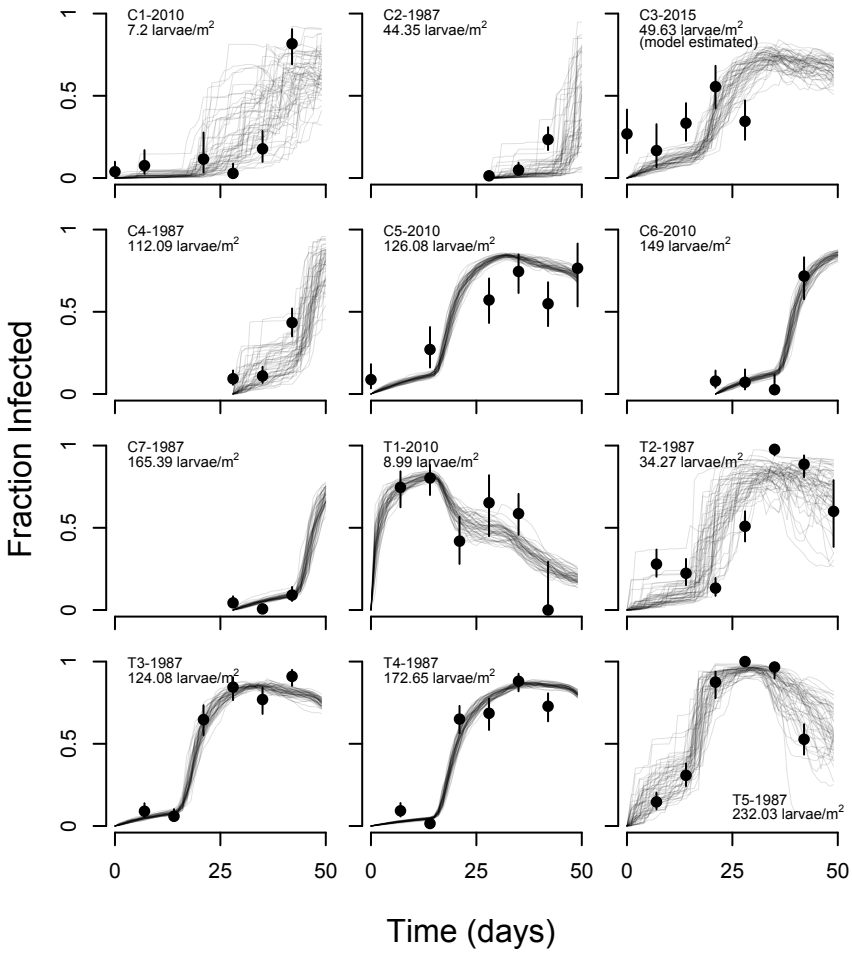

Figure 3: Stochastic realizations of the model that uses vague priors on all parameters, with symbols and labels as in fig. 2.

Taken together, these results provide a complicated answer to our original question: does transmission at a small-scale drive baculovirus epizootics at large scales? The similarity of our estimates of heterogeneity C between estimates based on experiments and estimates that take into account epizootics suggests that our experimental estimate of heterogeneity is close to the value of heterogeneity in nature. The effects of this heterogeneity are apparent in figs. 2 and 3. Relative to models without heterogeneity, models with heterogeneity tend to have lower infection rates at high host density, due to the dominating effects of resistant individuals, and higher infection rates at low host density, due to the presence of at least a few highly susceptible individuals

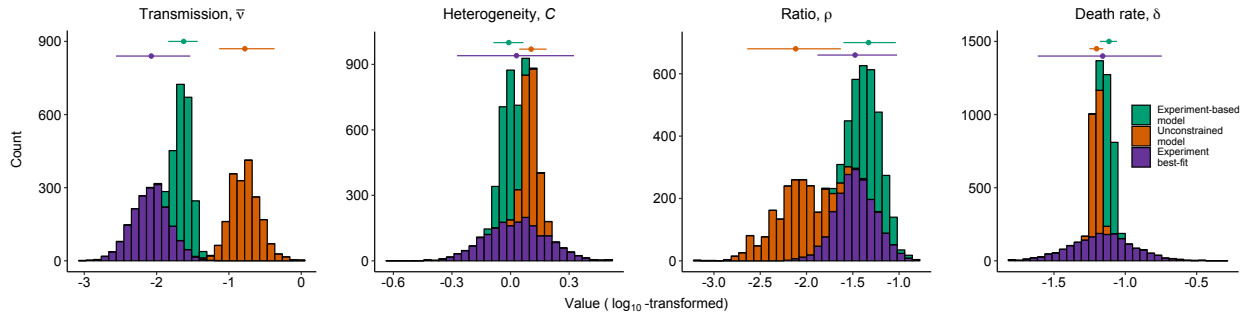

Figure 4: Comparison of posterior distributions for the 4 model parameters for which we have small-scale experimental estimates, the average transmission rate $\bar{v}$, the heterogeneity in transmission C, the ratio parameter ρ, and the death rate parameter δ. For each parameter, we compare the posterior marginal distribution from our experimental data (purple), to the posterior marginals when we fit models to the epizootic data. The latter distributions include the case in which we used experiment-based priors (green), and the case in which we used uninformed priors (orange). Points with error bars near the top of each panel show the median and the 95% credible interval in each case. Note that each panel has a different scale on its horizontal axis.

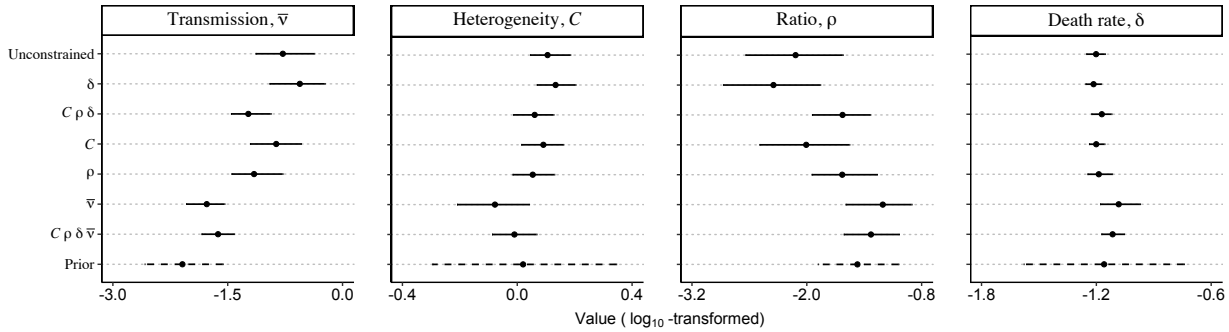

Figure 5: Summaries of the marginal posterior parameter estimates (columns) for all models (rows), compared to the experiment-based prior distributions derived from experiments (dashed lines). Dots are median values, while the horizontal bars show the 95% credible intervals. Note that each panel has a different scale on its horizontal axis.

Experiment-Based Priors On ...	Average Likelihood $\sum -\log(\hat{\bar{L}})$	Penalty Score $p\text{WAIC}_2$	WAIC	ΔWAIC
No parameters	**-197.33**	**5.95**	**406.58**	**0**
δ	**-197.05**	**6.34**	**406.79**	**0.21**
$C\ \rho\ \delta$	**-197.77**	**7.00**	**409.52**	**2.94**
C	**-197.09**	**7.71**	**409.61**	**3.03**
ρ	-198.38	7.44	411.64	5.06
$\bar{v}$	-199.20	7.08	412.57	5.99
$C\ \rho\ \delta\ \bar{v}$	-198.13	8.55	413.37	6.79
None, $C = 0^a$	-208.62	No Convergence		

Table 3: WAIC model selection for observational data. Models for which ΔWAIC$<\approx$ 3 are considered to be indistinguishable from the best model, and are therefore shown in bold face. [a]Because the model with no heterogeneity in transmission ($C = 0$) did not converge, the average likelihood for that model is a rough estimate based on non-converged MCMC samples.

(Dwyer et al., 1997). These effects are apparent in the epizootic data, in that infection rates were high across a broad range of densities. Because of this effect, models that do not account for heterogeneity provide poor fits to data from populations at either very low or very high densities (Table 3, also see Online Appendices). Mechanisms that affect variation in infection risk across individuals therefore appear to drive epizootics.

Our laboratory measure of the speed of kill, the inverse of δ, similarly appears to provide an accurate representation of speeds of kill in nature. This is at least somewhat surprising, given that baculovirus incubation times are sensitive to temperature (Cory and Myers, 2003), and given that temperatures in nature fluctuate, while temperatures in the speed-of-kill experiment were constant. Temperature variation in nature may therefore play only a minor role in epizootic dynamics. The apparent accuracy of our measure of the ratio parameter ρ is perhaps less surprising, given that ρ depends only on counts of occlusion bodies, which are unlikely to be affected by the

artificial conditions of the laboratory.

The large differences in posterior values of transmission $\bar{v}$, and the relatively worse WAIC score of models with experiment-based priors on $\bar{v}$, instead suggest that transmission rates may be affected by large-scale mechanisms. In the Discussion section, we discuss caveats to this conclusion, and we consider mechanisms that may drive transmission at larger scales. For now, we argue that large-scale phenomena likely affect the transmission of the tussock moth baculovirus, but that the ability of the model with experiment-based priors to explain most of the variability in the data (fig. 2), and the close agreement between the experimental and posterior estimates of heterogeneity in risk (fig. 4) nevertheless means that small-scale transmission mechanisms also play a clear role.

Discussion

The assumption that interactions between individual hosts determine infection and parasitization rates has been fundamental to studies of host-pathogen and host-parasitoid interactions for decades (Anderson and May, 1979; Varley et al., 1973). Meanwhile, as we mentioned, efforts to use models to explain large-scale pathogen or parasite dynamics have often relied on estimates of transmission rates or attack rates from laboratory data or large-scale data (Blackwood et al., 2013; Buhnerkempe et al., 2011; George et al., 2011; Murdoch et al., 2005). Given that our estimates of baculovirus transmission are instead based on small-scale field data, and given that the models with experiment-based priors are extrapolating over several orders of magnitude in spatial scale, the success of these models (fig. 2) provides important support for the conceptual foundations of disease ecology.

Our results nevertheless also suggest that large-scale transmission mechanisms affect baculovirus epizootics. As we explain in the Online Appendix, there are statistical complications involved in estimating transmission that cast some doubt on this conclusion. For the most part, however, these doubts suggest that the discrepancy between our experimental and epizootic-

based estimates of transmission $\bar{v}$ may not be as severe as fig. 4 suggests, rather than that there is no discrepancy. Our evidence for large-scale mechanisms thus provides an important caveat to our conclusions about small-scale mechanisms.

As we mentioned, there are several candidate large-scale mechanisms that may explain the discrepancy in our estimates of the transmission rate. First, observations by one of us (C. M.) have suggested that tussock moth larvae are clumped within trees, and this aggregation may increase infection rates relative to our experiments (Dwyer and Elkinton, 1993). Given that our estimates of over-dispersion levels are moderate, we suspect that these effects are modest, but more detailed data are clearly needed.

Second, the frequency of different tussock moth host trees varies spatially, such that Douglas fir, *Pseudotsuga menziesii*, is the dominant host tree species in British Columbia, while *Abies* species predominate in California and Nevada, with intermediate frequencies in Washington, Oregon, California, Idaho, Colorado, Arizona, and New Mexico (Shepherd et al., 1988). Given that our epizootic data were collected in British Columbia, Washington, Idaho, and Colorado, and given that baculovirus transmission can vary between insect host-tree species (Elderd et al., 2013), spatial variation in forest tree-species composition may also explain the discrepancy in our estimates of the transmission rate.

Third, the frequency of the two morphotypes of the baculovirus varies latitudinally, with high frequencies of *Op*MNPV in British Columbia, high frequencies of *Op*SNPV in New Mexico, and intermediate frequencies in Washington, Oregon, Idaho, and California (Williams et al., 2011). In our experiments, we tested only *Op*MNPV strains. Given that the two morphotypes are at least moderately diverged (Rohrmann et al., 1978), and given that we observed meaningful differences in transmission parameters even within *Op*MNPV strains, morphotype frequency variation between epizootics provides a third candidate large-scale mechanism to explain discrepancies in $\bar{v}$. Interactions between morphotypes and host-tree species provide yet a fourth candidate mechanism. Allowing for morphotype variation in our models was impractical, because the epizootic data do not include morphotype information, but understanding the consequences of this varia-

tion is another priority for future work.

A related point has to do with the role of stochasticity in the fit of the models. In the models with experiment-based priors on transmission, the median transmission rate on the prior is lower than values that would give a good fit to the epizootic data. In fitting those models to data from epizootics in low-density populations, the fitting routine therefore elevated the stochasticity in the low-density plots. These higher values of stochasticity ensure that the model output will be close to the data at least some of the time, an effect that is clearly apparent in fig. 2. Because of this effect, our median estimates of stochasticity in unsprayed populations fall with increases in the initial population density across epizootics (Online Appendix). This suggests that what we have treated as weather variation may instead be due to the chance events that befall individuals in small populations, an effect known as "demographic stochasticity" (Bolker, 2008). A better understanding of the effects of stochasticity might therefore substantially improve our understanding of baculovirus epizootics.

It is also important to point out that higher stochasticity by itself increases infection rates. This is because, in our models, stochasticity in transmission raises the rate at which both very low and very high transmission rates occur in our simulations, but higher transmission rates have disproportionately stronger effects (in the Online Appendices, we prove this assertion). This effect only became clear when we used experiment-based priors, emphasizing the usefulness of combining small-scale and large-scale data.

The importance of individual host variation in our results has general implications for the ecology of host-pathogen and host-parasitoid interactions. First, in infectious-disease modeling, host heterogeneity is typically only considered in studies of sexually transmitted infections (Keeling and Rohani, 2008). We suspect that this lack of consideration of host heterogeneity results from a lack of tests of models that include host heterogeneity, rather than from an actual lack of host heterogeneity in nature. From that perspective, it is worth noting that, in arguing for effects of an invulnerable host stage on host-parasitoid dynamics, Murdoch et al. (2005) similarly emphasized the necessity of using large-scale data to test models parameterized with small-scale

data. Given that an invulnerable stage and host variation in infection risk are simply two forms of population structure, detecting the effects of host variation on non-sexually transmitted infections in other hosts may generally require estimation of model parameters from individual-scale data. Although such estimates are often unavailable for vertebrate pathogens, an alternative approach may come from recent efforts to estimate the force of infection, of which the transmission rate is a component, from measurements of antibody kinetics in individual hosts (Pepin et al., 2017).

In theories of host-parasitoid interactions, models similar to ours have been used to argue that heterogeneity in risk explains why introduced parasitoids often maintain populations of their hosts at low, stable densities (Hassell et al., 1991; Pacala and Hassell, 1991). For the most part, however, empiricists have discarded these models in favor of models that instead invoke the presence of an invulnerable adult stage in the host (Murdoch et al., 2006). The failure of the original theory was sufficiently dramatic that it has fueled discussion about whether ecological theory has ever been of value in biological control (McEvoy, 2018; Mills and Kean, 2010).

Our results provide an alternative view. First, the agreement between our experimental and posterior estimates of heterogeneity in risk is strong evidence that host variation plays a key role in epizootics of the tussock moth baculovirus (fig. 2). Previous work with the gypsy moth baculovirus similarly supported the models that we use here, albeit without allowing for parameter uncertainty (Dwyer et al., 1997). Because the tussock moth and the gypsy moth are representative of a broad group of outbreaking Lepidoptera that are affected by baculoviruses (Moreau and Lucarotti, 2007), host heterogeneity in infection risk may play a more general role in insect population dynamics than has been previously suggested (Murdoch et al., 2006).

The specific values of our estimates of heterogeneity in risk C are also broadly relevant for insect ecology. The "$\mathrm{CV}^2 > 1$ rule" of insect ecology defines an upper limit on heterogeneity in host-parasitoid (Hassell et al., 1991) and host-pathogen models (Dwyer et al., 2000), above which the host population will be stable. As (fig. 4) shows, a substantial fraction of our posterior estimates of C are greater than 1, and for the model with vague priors, the lower bound on

the 95% credible interval is above 1. Our estimates of C therefore suggest that tussock moth populations should not have outbreaks, a prediction that is at odds with observations of tussock moth outbreaks in nature (Mason, 1996). The $CV^2 > 1$ rule, however, assumes that there is no selection on host resistance, whereas allowing for selection and a fecundity tradeoff again leads to realistic cycles (Páez et al., 2017). Natural selection may therefore play a key role in tussock moth population cycles.

More practically, our work shows that, contrary to the failure of models with continuously distributed heterogeneity in parasitoid-based biological control (McEvoy, 2018), such models may be widely useful in pathogen-based or "microbial" control (Hunter-Fujita et al., 1998). Indeed, in both the Douglas-fir tussock moth (Scott and Spiegel, 2002) and several other insects (Moreau and Lucarotti, 2007; Podgwaite, 1985; Wollam et al., 1978), baculovirus epizootics in unsprayed control plots have often occurred at host densities that researchers believed were too low to support epizootics. As our results demonstrate, host heterogeneity can cause epizootics to occur over an unexpectedly broad range of host densities (Dwyer et al., 1997). It is important to add that, in the insect pathology literature, there is a long tradition of explaining epizootics by invoking complex mechanisms other than density (Fuxa and Tanada, 1987). A deeper understanding of the effects of host and pathogen densities on baculovirus dynamics may therefore improve control strategies (Brown, 1987; Moscardi, 1999; Podgwaite, 1985).

Our Bayesian approach has the advantage that it allowed us to test the extent to which our small-scale, experimental data help us to understand large-scale epizootic data. We therefore echo Restif et al. (2012)'s argument that Bayesian methods can allow for deeper insight into disease dynamics. More conventional maximum-likelihood methods have driven the development of flexible "plug-and-play" software, which has been used to fit complex models like ours to data (Ionides et al., 2006, 2015; King et al., 2016), leading to important insights into disease dynamics (King et al., 2016; Martinez et al., 2016; Ranjeva et al., 2017). Maximum likelihood methods, however, do not allow for comparison of models that do and do not take into account prior information, thus preventing comparison of models that do and do not take into account exper-

imental data. A Bayesian version of particle filtering shows great promise, but sometimes fails to converge on the best parameters (Ionides et al., 2015). The computational methods that we present here may therefore be of general usefulness.

Acknowledgments

We are grateful for the support of dedicated and talented field technicians: Ruby An, Kate Lynne Logan, Rachel Hosman, Hannah Koch, Jenni Novak, Katherine Sirianni, Jeffrey Thorburn, Alison Hunter, Cara Skalisky, Alyssa Taylor, Jason Sims, and Rita Bennett. Roy Magelssen provided information on spray projects in general and some field support for the 2010 project on the Methow Ranger District. Natural epizootic data were provided with the assistance of Tom Eckberg, Idaho Department of Lands and by Rebecca Powell, Forest Health Protection, Rocky Mountain Region. JRM was funded by a US Department of Agriculture (USDA) National Institute of Food and Agriculture (NIFA) Postdoctoral Fellowship (2014-67012-22272). Additional work was funded by the Okanogan-Wenatchee National Forest (Methow Ranger District), and a grant to KMP and GD from the USDA Forest Service Pesticide Impacts Assessment Program. Helpful feedback was provided by Iral Ragenovich, USDA Forest Service, Region 6 Forest Health Protection. Imre Otvos kindly provided the epizootic data from 1987. M.E. Martignoni provided important encouragement to G.D. at a crucial career juncture decades ago.

Literature Cited

Anderson, R. M., and R. M. May. 1979. Population biology of infectious diseases: Part i. Nature 280:361–367.

———. 1992. Infectious diseases of humans: dynamics and control. Oxford University Press, Oxford.

Blackwood, J. C., D. G. Streicker, S. Altizer, and P. Rohani. 2013. Resolving the roles of immunity, pathogenesis, and immigration for rabies persistence in vampire bats. Proceedings of the National Academy of Sciences 110:20837–20842.

Bolker, B. M. 2008. Ecological models and data in R. Princeton University Press.

Box, G. 1979. Robustness in the strategy of scientific model building. Pages 202–236 *in* R. L. Launer and G. N. Wilkinson, eds. Robustness in Statistics. Academic Press, N.Y.

Brown, G. 1987. Modeling. Pages 43–71 *in* J. Fuxa and Y. Tanada, eds. Epizootiology of Insect Diseases. John Wiley & Sons, New York, NY.

Buhnerkempe, M. G., R. J. Eisen, B. Goodell, K. L. Gage, M. F. Antolin, and C. T. Webb. 2011. Transmission shifts underlie variability in population responses to yersinia pestis infection. PloS one 6:e22498.

Burand, J. P., and E. J. Park. 1992. Effect of nuclear polyhedrosis-virus infection on the development and pupation of gypsy-moth larvae. Journal of Invertebrate Pathology 60:171–175.

Cory, J. S., and K. Hoover. 2006. Plant-mediated effects in insect-pathogen interactions. Trends in Ecology and Evolution 21:278–286.

Cory, J. S., and J. H. Myers. 2003. The ecology and evolution of insect baculoviruses. Annual Reviews of Ecology and Systematics 34:239–272.

Cox, D. R., and E. Snell. 1989. Analysis of binary data. Routledge.

Dwyer, G. 1991. The effects of density, stage and spatial heterogeneity on the transmission of an insect virus. Ecology 72:559–574.

———. 1992. On the spatial spread of insect pathogens - theory and experiment. Ecology 73:479–494.

Dwyer, G., J. Dushoff, J. S. Elkinton, and S. A. Levin. 2000. Pathogen-driven outbreaks in forest defoliators revisited: Building models from experimental data. American Naturalist 156:105–120.

Dwyer, G., and J. S. Elkinton. 1993. Using simple-models to predict virus epizootics in gypsy-moth populations. Journal Of Animal Ecology 62:1–11.

———. 1995. Host dispersal and the spatial spread of insect pathogens. Ecology 76:1262–1275.

Dwyer, G., J. S. Elkinton, and J. P. Buonaccorsi. 1997. Host heterogeneity in susceptibility and disease dynamics: Tests of a mathematical model. American Naturalist 150:685–707.

Eakin, L., M. Wang, and G. Dwyer. 2015. The effects of the avoidance of infectious hosts on infection risk in an insect-pathogen interaction. Am. Nat. 185:pp. 100–112.

Elderd, B., V. Dukic, and G. Dwyer. 2006. Uncertainty in predictions of disease spread and public-health responses to bioterrorism and emerging diseases. Proceedings of the National Academy of Sciences 103:15693–15697.

Elderd, B. D. 2013. Developing models of disease transmission: Insights from ecological studies of insects and their baculoviruses. PLoS Pathogens 9.

Elderd, B. D., J. Dushoff, and G. Dwyer. 2008. Host-pathogen interactions, insect outbreaks, and natural selection for disease resistance. The American Naturalist 172:829–842.

Elderd, B. D., B. J. Rehill, K. J. Haynes, and G. Dwyer. 2013. Induced plant defenses, host–pathogen interactions, and forest insect outbreaks. Proc. Natl. Acad. Sci. 110:14978–14983.

Fleming-Davies, A. E., V. Dukic, V. Andreasen, and G. Dwyer. 2015. Effects of host heterogeneity on pathogen diversity and evolution. Ecology Letters 18:1252–1261.

Fuller, E., B. D. Elderd, and G. Dwyer. 2012. Pathogen persistence in the environment and insect-baculovirus interactions: Disease-density thresholds, epidemic burnout, and insect outbreaks. Am. Nat. 179:pp. E70–E96.

Fuxa, J. R., and Y. Tanada. 1987. Epizootiology of insect diseases. Wiley.

Gelman, A., J. B. Carlin, H. S. Stern, D. B. Dunson, A. Vehtari, and D. B. Rubin. 2014. Bayesian Data Analysis, Third Edition. Chapman & Hall/CRC Press. New York, NY.

George, D. B., C. T. Webb, M. L. Farnsworth, T. J. O'Shea, R. A. Bowen, D. L. Smith, T. R. Stanley, L. E. Ellison, and C. E. Rupprecht. 2011. Host and viral ecology determine bat rabies seasonality and maintenance. Proceedings of the National Academy of Sciences 108:10208–10213.

Grimm, V., E. Revilla, U. Berger, F. Jeltsch, W. M. Mooij, S. F. Railsback, H.-H. Thulke, J. Weiner, T. Wiegand, and D. L. DeAngelis. 2005. Pattern-oriented modeling of agent-based complex systems: lessons from ecology. science 310:987–991.

Grove, M. J., and K. Hoover. 2007. Intrastadial developmental resistance of third instar gypsy moths (*Lymantria dispar* l.) to *L. dispar* nucleopolyhedrovirus. Biological Control 40:355–361.

Han, X., and P. E. Kloeden. 2017. Random Ordinary Differential Equations and Their Numerical Solution. Springer.

Hassell, M., R. May, S. Pacala, and P. Chesson. 1991. The persistence of host-parasitoid associations in patchy environments. i. a general criterion. The American Naturalist 138:568–583.

Hughes, K., and R. Addison. 1970. Two nuclear polyhedrosis viruses of Douglas-fir tussock moth. Journal of Invertebrate Pathology 16:196–&.

Hunter-Fujita, F. R., P. F. Entwistle, H. F. Evans, and N. E. Crook. 1998. Insect viruses and pest management. John Wiley and Sons: Somerset, New Jersey.

Ionides, E. L., C. Bretó, and A. A. King. 2006. Inference for nonlinear dynamical systems. Proceedings of the National Academy of Sciences of the United States of America 103:18438–43.

Ionides, E. L., D. Nguyen, Y. Atchadé, S. Stoev, and A. A. King. 2015. Inference for dynamic and latent variable models via iterated, perturbed Bayes maps. Proceedings of the National Academy of Sciences 112:719–724.

Kareiva, P., and G. Odell. 1987. Swarms of predators exhibit" preytaxis" if individual predators use area-restricted search. The American Naturalist 130:233–270.

Keeling, M. J., and P. Rohani. 2008. Modeling Infectious Diseases in Humans and Animals. Princeton University Press.

Keeling, M. J., M. E. Woolhouse, D. J. Shaw, L. Matthews, M. Chase-Topping, D. T. Haydon, S. J. Cornell, J. Kappey, J. Wilesmith, and B. T. Grenfell. 2001. Dynamics of the 2001 uk foot and mouth epidemic: stochastic dispersal in a heterogeneous landscape. Science 294:813–817.

King, A. A., D. Nguyen, and E. L. Ionides. 2016. Statistical Inference for Partially Observed Markov Processes via the R Package pomp. Journal of Statistical Software 69.

Lance, D., J. Elkinton, and C. Schwalbe. 1986. Feeding rhythms of gypsy moth larvae: effect of food quality during outbreaks. Ecology 67:1650–1654.

Levin, S. A. 1992. The problem of pattern and scale in ecology: the robert h. macarthur award lecture. Ecology 73:1943–1967.

Longini, I. M., A. Nizam, S. Xu, K. Ungchusak, W. Hanshaoworakul, D. A. Cummings, and M. E. Halloran. 2005. Containing pandemic influenza at the source. Science 309:1083–1087.

Martignoni, M. E. 1999. History of tm biocontrol-1, the first registered virus-based produced for control of a forest insect. The American Entomologist 45:30–37.

Martinez, P. P., A. A. King, M. Yunus, A. Faruque, and M. Pascual. 2016. Differential and enhanced response to climate forcing in diarrheal disease due to rotavirus across a megacity of the developing world. Proceedings of the National Academy of Sciences 113:4092–4097.

Mason, R. 1996. Dynamic behavior of Douglas-fir tussock moth populations in the Pacific northwest. Forest Science 42:182–191.

Mason, R., and T. Torgersen. 1983. Mortality of larvae in stocked cohorts of the Douglas-fir tussock moth, *Orgyia pseudotsugata* (Lepidoptera: Lymantriidae). Canadian Entomologist 115:1119–1127.

McCallum, H., N. Barlow, and J. Hone. 2001. How should pathogen transmission be modelled? Trends in ecology & evolution 16:295–300.

McCullagh, P., and J. Nelder. 1989. Generalized Linear Models. Chapman & Hall, Boca Raton, FL.

McEvoy, P. B. 2018. Theoretical contributions to biological control success. BioControl pages 1–17.

Mihaljevic, J., K. Polivka, C. Mehmel, V. Dukic, and G. Dwyer. 2019. Using mechanistic transmission models to guide microbial control programs. Biological Control in prep.

Miller, L. K. 1997. The baculoviruses. Plenum Press.

Mills, N. J., and J. M. Kean. 2010. Behavioral studies, molecular approaches, and modeling: methodological contributions to biological control success. Biological Control 52:255–262.

Moreau, G., and C. J. Lucarotti. 2007. A brief review of the past use of baculoviruses for the management of eruptive forest defoliators and recent developments on a sawfly virus in canada. Forestry Chronicle 83:105–112.

Moscardi, F. 1999. Assessment of the Application of Baculoviruses for Control of Lepidoptera. Annual Review of Entomology 44:257–289.

Murdoch, W., C. J. Briggs, and S. Swarbrick. 2005. Host suppression and stability in a parasitoid-host system: experimental demonstration. Science 309:610–613.

Murdoch, W. W., S. L. Swarbrick, and C. J. Briggs. 2006. Biological control: lessons from a study of california red scale. Population Ecology 48:297–305.

Myers, J. H. 1988. Can a general hypothesis explain population cycles of forest lepidoptera? Advances in Ecological Research 18:179–242.

Øksendal, B. 2003. Stochastic differential equations. Pages 65–84 *in* Stochastic differential equations. Springer.

Otvos, I., J. Cunningham, and R. Alfaro. 1987. Aerial Application Of Nuclear Polyhedrosis-Virus Against Douglas-Fir Tussock Moth, Orgyia-Pseudotsugata (Mcdunnough) (Lepidoptera, Lymantriidae).2. Impact 1-Year And 2 Years After Application. Canadian Entomologist 119:707–715.

Otvos, I. S., J. C. Cunningham, and L. M. Friskie. 1987. Aerial application of nuclear polyhedrosis virus against douglas-fir tussock moth, *Orgyia pseudostugata* (Mcdunnough) (Lepidoptera: Lymantriidae). 1. impact in the year of application. Canadian Entomologist 119:697–706.

Pacala, S., and M. Hassell. 1991. The persistence of host-parasitoid associations in patchy environments. ii. evaluation of field data. The American Naturalist 138:584–605.

Páez, D., V. Dukic, J. Dushoff, A. Fleming-Davies, and G. Dwyer. 2017. Effects of pathogen exposure on life-history variation in the gypsy moth (lymantria dispar). The American Naturalist accepted pending minor revision.

Pascual, M. A., and P. Kareiva. 1996. Predicting the outcome of competition using experimental data: maximum likelihood and bayesian approaches. Ecology 77:337–349.

Pepin, K. M., S. L. Kay, B. D. Golas, S. S. Shriner, A. T. Gilbert, R. S. Miller, A. L. Graham, S. Riley, P. C. Cross, M. D. Samuel, et al. 2017. Inferring infection hazard in wildlife populations by linking data across individual and population scales. Ecology Letters 20:275–292.

Podgwaite, J. 1985. Strategies for field use of baculoviruses. Pages 775–799 *in* K. Maramorosch and K. Sherman, eds. Viral Insecticides for Biological Control. Academic Press, Orlando, Florida.

Polivka, K., G. Dwyer, and C. Mehmel. 2017. Environmental persistence of a pathogen used in microbial insect control. Research Note PNW-RN-573, Pacific Northwest Research Station, USDA Forest Service.

Press, W. H., S. A. Teukolsky, W. T. Vetterling, and B. P. Flannery. 1992. Numerical recipes in C, vol. 2. Cambridge university press Cambridge.

Ranjeva, S. L., E. B. Baskerville, V. Dukic, L. L. Villa, E. Lazcano-Ponce, A. R. Giuliano, G. Dwyer, and S. Cobey. 2017. Recurring infection with ecologically distinct hpv types can explain high prevalence and diversity. Proceedings of the National Academy of Sciences page 201714712.

Restif, O., D. T. Hayman, J. R. Pulliam, R. K. Plowright, D. B. George, A. D. Luis, A. A. Cunningham, R. A. Bowen, A. R. Fooks, T. J. O'Shea, et al. 2012. Model-guided fieldwork: practical guidelines for multidisciplinary research on wildlife ecological and epidemiological dynamics. Ecology letters 15:1083–1094.

Rohrmann, G., R. McParland, M. Martignoni, and G. Beaudreau. 1978. Genetic relatedness of 2 nucleopolyhedrosis viruses pathogenic for *Orgyia pseudotsugata*. Virology 84:213–217.

Rohrmann, G. F. 2014. Baculovirus nucleocapsid aggregation (MNPV vs SNPV): an evolutionary strategy, or a product of replication conditions? Virus Genes 49:351–357.

Ross, S. 2002. Simulation, 3rd. Edition. Academic Press, New York.

Schindelin, J., C. T. Rueden, M. C. Hiner, and K. W. Eliceiri. 2015. The ImageJ ecosystem: An open platform for biomedical image analysis. Molecular Reproduction and Development 82:518–529.

Scott, D., and L. Spiegel. 2002. One and two year follow-up evaluation of TM Biocontrol-1 treatments to suppress Douglas-fir tussock moth in the Blue Mountains of northeastern Oregon and southeastern Washington. Technical Report BMPMSC-02-02, USDA Forest Service, Pacific Northwest Region.

Shepherd, R., D. Bennett, J. Dale, S. Tunnock, R. Dolph, and R. Thier. 1988. Evidence of synchronized cycles in outbreak patterns of Douglas-fir tussock moth, *Orgyia pseudotsugata* (McDunnough) (Lepidoptera:Lymantriidae). Memoirs of the Entomological Society of Canada pages 107–121.

Shepherd, R. F., I. S. Otvos, R. J. Chorney, and J. C. Cunningham. 1984. Pest-management of Douglas-fir tussock moth (Lepidoptera: Lymantriidae) - prevention of an outbreak through early treatment with a nuclear polyhedrosis-virus by ground and aerial applications. Canadian Entomologist 116:1533–1542.

Thompson, C., and D. Scott. 1979. Production And Persistence Of The Nuclear Polyhedrosis-Virus Of The Douglas-Fir Tussock Moth, Orgyia-Pseudotsugata (Lepidoptera, Lymantriidae), In The Forest Ecosystem. Journal Of Invertebrate Pathology 33:57–65.

Varley, G. C., G. R. Gradwell, and M. P. Hassell. 1973. Insect population ecology: an analytical approach. Blackwell Scientific Publications: Oxford.

Williams, H. L., K. S. Monge-Monge, I. S. Otvos, R. Reardon, and I. Ragenovich. 2011. Genotypic variation among Douglas-fir tussock moth nucleopolyhedrovirus (OpNPV) isolates in the western United States. Journal of Invertebrate Pathology 108:13–21.

Wollam, J. D., W. G. Yendol, and F. B. Lewis. 1978. Evaluation of aerially-applied nuclear polyhedrosis virus for suppression of the gypsy moth, Lymantria dispar L. Forest Service Research Paper NE-396:8 p.